PHYSICAL REVIEW D VOLUME 44, NUMBER 2 15 JULY 1991

Quark- and gluon-jet emission from primordial black holes. II. The emission over the black-hole lifetime

Jane H. MacGibbon*
Institute of Astronomy, University of Cambridge, Cambridge, England CB3 0HA
(Received 13 December 1990)

The emission produced over the lifetime of black holes with masses less than $M_* \simeq 4-6\times10^{14}$ g is investigated by convolving the Hawking emission formulas with a Monte Carlo QCD jet code. Such emission may be astrophysically important if, for example, holes form from initial density perturbations in the early Universe. The quark and gluon decay products contribute significantly to the M_* emission and dominate the lifetime emission from holes with initial masses less than about 10^{14} g. The M_* emission shows little sensitivity to the uncertainties in particle-physics models around 100–300 MeV and above 100 GeV. A more precise determination of the mass of a primordial black hole which just expires today is also given as a function of the cosmological matter density and Hubble constant.

I. INTRODUCTION

Many scenarios of the early Universe have been proposed over the last 25 years in which primordial black holes (PBH's) form [1]. Such mechanisms include PBH creation from initial density inhomogeneities [2], phase transitions [3], a softening of the Universe's equation of state [4] and the collapse of cosmic strings [5]. Thus the existence or nonexistence of PBH's should give important information on various theories of the early Universe. Only holes with masses greater than $M_* \simeq 4-6\times10^{14}$ g, however, will have survived until the present day [6]. PBH's with smaller initial masses will have evaporated completely via Hawking radiation [7]. The Hawking emission from the surviving holes presents the best method for the detection of PBH's. Holes with initial masses slightly greater than M_* have masses today of $M < M_*$ and a number distribution of $dn/dM \propto M^2$, independent of their formation mechanism [8]. Holes with masses much greater than M_* lose little mass over the lifetime of the Universe and their initial mass distribution should be unchanged. If PBH's form from scale-invariant initial density perturbations (the most natural scenario), the initial PBH mass spectrum falls off as $dn/dM_i \propto M_i^{-1-(1+3\gamma)/(1+\gamma)}$ where $p=\gamma\rho$ is the equation of state of the formation epoch [9]. Hence the most interesting emission today is likely to come from M_* holes.

Holes of mass M_* are close to the threshold for the emission of quarks and gluons. In a previous paper [10], MacGibbon and Webber updated Page's and Hawking's original work [11-13], on the instantaneous electron, neutrino and photon emission from PBH's, to include QCD particle decays. For this, they used the Monte Carlo jet codes BIGWIG and HERWIG. They found that particle decays dominate the instantaneous flux from black holes with masses less than about 10^{14} g. In this paper, their approach is extended to investigate the emission from an M_* black hole over its lifetime. A more exact calculation of M_*, the mass of a black hole whose lifetime equals the present age of the Universe, is also given and the sensitivity of the lifetime emission to M_* and the uncertainties in particle models around the quark-hadron transition Λ_{QH} and above 100 GeV is explored. The M_* emission forms the basis for the calculation of the photon and cosmic-ray backgrounds emitted by a PBH distribution. These backgrounds and their astrophysical consequences are derived elsewhere [14,15]. MacGibbon and Carr find that, including QCD decays, the emission from PBH's created by scale-invariant initial density perturbations may explain or contribute significantly to the observed extragalactic photon and interstellar electron, positron and antiproton spectra between 0.1–1 GeV, provided that PBH's cluster to the same degree as other matter in the galactic halo. They require a present density in PBH's of $\Omega_{PBH} \simeq 10^{-8}$, in units of the critical density. On the other hand, bursts from individual PBH's are extremely unlikely [16] to be observed in the standard evaporation model, unless a Hagedorn-type exponential growth in particle states occurs as the black-hole temperature approaches Λ_{QH}.

The structure of the paper is as follows. Section II reviews Hawking radiation; Secs. III and IV discuss the mass loss and lifetime of a black hole; Secs. V and VI discuss the emission over the lifetime and the analytic approximations to the spectra; Sec. VII describes the numerical method used to generate the emission; and Sec. VIII presents the numerical results. Our attention is generally restricted to the standard experimentally verified elementary particles and the top quark. Unless specified, we use units in which mass M is in grams and temperature T is in GeV. "Primary emission" denotes those particles directly emitted by the hole, and not those created by the decay of the emission.

II. HAWKING RADIATION

Let us consider an uncharged, nonrotating Schwarzshild black hole of mass M. Hawking showed that such a hole emits particles with spin s and total ener-

gy between $(Q, Q+dQ)$ at a rate [6,7]

$$d\dot{N}=\frac{\Gamma_s dQ}{2\pi\hbar}\left[\exp\left[\frac{8\pi GQM}{\hbar c^3}\right]-(-1)^{2s}\right]^{-1} \quad (1)$$

per degree of particle freedom. The dimensionless absorption probability for the emitted species Γ_s is in general a function of Q, M and the particle's internal degrees of freedom and rest mass. $\Gamma_s(M,Q)$ approaches $27G^2M^2Q^2/\hbar^2c^6$ as $Q\to\infty$ but falls off more quickly as $Q\to 0$, with the higher spins producing the stronger cutoffs [12]. Any nonzero electric charge and angular momentum of the hole or particle has a negligible effect at the black-hole masses that we are considering [10,13,17]. Equation (1) breaks down when M approaches the Planck mass.

The Hawking radiation mimics thermal emission from a blackbody with a finite size and a temperature of

$$kT=\frac{\hbar c^3}{8\pi GM}=1.06\left[\frac{M}{10^{13}\text{ g}}\right]^{-1}\text{ GeV} . \quad (2)$$

Summing over helicity states, the peak nondecaying primary flux is (Ref. [12]) $d\dot{N}/dQ=9.39\times10^{21}$ GeV^{-1} sec^{-1} at $MQ\simeq4.26\times10^{13}$ g GeV in electrons and positrons and $d\dot{N}/dQ=1.38\times10^{21}$ GeV^{-1} sec^{-1} at $MQ\simeq6.12\times10^{13}$ g GeV in photons. The peak power is $dP/dQ=4.25\times10^{22}/(M/10^{13}\text{ g})$ sec^{-1} at $MQ\simeq4.74\times10^{13}$ g GeV in $e^{\pm}$ and $dP/dQ=8.62\times10^{21}/(M/10^{13}\text{ g})$ sec^{-1} at $MQ\simeq6.38\times10^{13}$ g GeV in photons. The average direct π^0 energy [18] (approximately the energy of peak $s=0$ power) is $\bar{E}_{s=0}=2.81kT$ in the relativistic limit. Thus we see that most emitted particles are relativistic and produced copiously once T reaches their rest mass μ. Nonrelativistic corrections to Γ_s need only be applied when the flux and power peak around μ. Equation (1) also implies that any species is emitted to some degree at all T. In our approach, the black hole directly emits those particles which appear elementary on the scale of the radiated energy and the hole's dimensions, rather than composite particles. When Q exceeds $\Lambda_{\rm QH}\simeq250$–$300$ MeV, quarks and gluons are emitted, which then fragment into further quarks and gluons. These cluster into composite hadrons on distances greater than about $1/\Lambda_{\rm QH}$ (appropriately Lorentz transformed). As verified in Ref. [10] and references therein, this process is consistent with our current understanding of accelerator physics. It is analogous to the decay of quark and gluon jets in e^+e^- annihilation. Similarly, if 100 MeV $\lesssim Q\lesssim\Lambda_{\rm QH}$, pions should be emitted as primary noncomposite particles, independently on the scale of their interactions. In any particle model, the form of the cutoff in hadron production around the $\Lambda_{\rm QH}$ is uncertain. This uncertainty is at least comparable with the nonrelativistic corrections to Γ_s around $\Lambda_{\rm QH}$. However, the cutoff in Γ_s at rest mass, together with the huge increase in degrees of freedom and decay products for quarks and gluons, ensure that the precise behavior near $\Lambda_{\rm QH}$ is not needed when calculating the lifetime emission from an M_* hole. This is confirmed in Sec. VIII.

We proceed by convolving Eq. (1) with functions to describe the decay of the primary emission into photons, neutrinos, electrons, positrons, protons, and antiprotons. (These are the particles which are stable on astrophysical time scales). If $dg_{jX}(Q,E)/dE$ is the relative number of X particles with energy E produced by parent j with energy Q, such that (i) $dg_{jj}(Q,E)/dE=\delta(Q-E)$ and (ii) $\int[dj_{jX}(Q,E)/dE]dE=$ total number of X particles created by j, the flux of X particles from the hole is

$$\frac{d\dot{N}_X}{dE}=\sum_j\int_{Q=E}^{Q=\infty}\frac{\Gamma_j(Q,T)}{2\pi\hbar}\left[\exp\left[\frac{Q}{kT}\right]-(-1)^{2s_j}\right]^{-1}\times\frac{dg_{jX}(Q,E)}{dE}dQ . \quad (3)$$

Here we sum over all contributing species and their degrees of freedom. The $T=0.3$–100 GeV flux has the following features [10]: (a) peaks below $E\simeq5$ MeV in the $e^{\pm}$ and $\nu\bar{\nu}$ spectra from neutron β decay in the jets: (b) peaks around $E\simeq0.01$–10 GeV in the $e^{\pm}$, γ, and $\nu\bar{\nu}$ spectra from roughly equal numbers of jet π^+, π^-, and π^0 (the pion decays dominate the total flux); and (c) relatively insignificant peaks at $E\simeq5T$ in the $e^{\pm}$, γ, and $\nu\bar{\nu}$ spectra from the nondecaying emission. The $p\bar{p}$ spectrum, which is entirely jet produced, has a slope of about $E^{0.5}$ at low energies, an E^{-1} slope at 0.3 GeV $\lesssim E\lesssim T$, and an exponential cutoff at high energies. Particles are generated approximately in the ratio 2% $p\bar{p}$, 20% $e^{\pm}$, 22% γ, and 56% $\nu\bar{\nu}$. Equal numbers of a particle and its antiparticle are emitted at these temperatures.

III. MASS LOSS

By conservation of energy, the emission of a particle with total energy Q should decrease the black-hole mass by Q/c^2. (Strictly, proof of this decrease requires a back-reaction calculation, techniques for which have yet to be furnished). Summing over all emitted species, the mass loss rate is

$$\frac{dM}{dt}=-\sum_j\frac{1}{2\pi\hbar}\int\Gamma_j\left[\exp\left[\frac{8\pi GQM}{\hbar c^3}\right]-(-1)^{2s_j}\right]^{-1}\times\frac{Q}{c^2}dQ . \quad (4)$$

We integrate over $0\le Q<\infty$ for massless particles and $\mu_j\le Q<\infty$ for massive particles. Equation (4) can be written for general M as

$$\frac{dM}{dt}=-5.34\times10^{25}f(M)M^{-2}\text{ g sec}^{-1} , \quad (5)$$

where $f(M)$, a function of the number of emitted species, is normalized to unity for $M\gg10^{17}$ g holes emitting only massless photons and three kinds of neutrinos. Since the integration limits and Γ_s depend on M and μ for massive particles, f is not strictly independent of M for a fixed number of species. Integrating the power carried by each species over Q [see Eq. (10) in Ref. [10]], the relativistic contributions to $f(M)$ per degree of particle freedom are

$$f_{s=0}=0.267,\ f_{s=1}=0.060,\ f_{s=3/2}=0.020,$$
$$f_{s=2}=0.007, \tag{6}$$
$$f_{s=1/2}=\begin{cases}0.147 & \text{uncharged,}\\ 0.142 & \text{electric charge}=\pm e\ .\end{cases}$$

Massless $s=2$ gravitons would increase (Ref. [12]), $f(M)$ by less than 1.4% but we shall confine ourselves here to the experimentally verified particles and the top quark. Each $s=1/2$ quark flavor has 12 degrees of freedom, the $s=1$ gluon has 16 and the $s=0$ pion has 3 states with $m_{\pi^0}\simeq 135$ MeV and $m_{\pi^\pm}\simeq 140$ MeV. A 5×10^{14} g $\ll M \ll 10^{17}$ g hole emitting electrons, positrons, photons, and neutrinos initially has $f(M)=1.569$. As M decreases, the hole begins to emit $q_u,q_d,q_s,q_c,q_b,q_t,\mu^\pm,\tau^\pm$, and gluons. To account for the gradual increase in $f(M)$ as the peak power approaches each new mass threshold, we can approximate $f(M)$ by

$$f(M)=1.569+0.569\left[\exp\left[\frac{-M}{\beta_{s=1/2}M_\mu}\right]+3\exp\left[\frac{-M}{\beta_{s=1/2}M_u}\right]+3\exp\left[\frac{-M}{\beta_{s=1/2}M_d}\right]+3\exp\left[\frac{-M}{\beta_{s=1/2}M_s}\right]\right.$$
$$\left.+3\exp\left[\frac{-M}{\beta_{s=1/2}M_c}\right]+\exp\left[\frac{-M}{\beta_{s=1/2}M_\tau}\right]+3\exp\left[\frac{-M}{\beta_{s=1/2}M_b}\right]+3\exp\left[\frac{-M}{\beta_{s=1/2}M_t}\right]\right]$$
$$+0.963\exp\left[\frac{-M}{\beta_{s=1}M_g}\right], \tag{7}$$

for 10^{12} g $\lesssim M \ll 10^{17}$ g. In Eq. (7), M_j is the mass of a hole whose temperature equals the rest mass of the jth species, μ_j, and β_{s_j} is defined so that the power of an $M=\beta_{s_j}M_j$ hole peaks at μ_j. Using Ref. [12] and Eqs. (9) and (11) in Ref. [10], we have

$$\beta_{s=0}=2.66,\ \beta_{s=1/2}=4.53,\ \beta_{s=1}=6.04,\ \beta_{s=2}=9.56 \tag{8}$$

The values for other spins can be estimated by plotting the logarithm of the energy at peak power as a function of s. Table I displays our values for μ_j, $\beta_j M_j$, and T_j/β_j. The effective quark masses are the "constituent" quark masses whose sums, allowing for spin-spin interactions, explain the hadron masses. Our effective gluon "mass," $m_g\simeq 600$–700 MeV, is the infrared cutoff in the relevant QCD renormalization (see, for example, Ref. [19]). These effective masses are only known to one or two significant figures. The top quark, as yet unobserved, must have a mass above 89 GeV at the 95% confidence level [20]. We assume that the $f(M)$ contribution per quark or gluon degree of freedom is the same as that per $e^\pm$ or photon degree, respectively. Since the electric charge is $\pm 2/3$ for $q_{u,c,t}$ and $\pm 1/3$ for $q_{d,s,b}$, and the flux decreases slightly with particle charge [13], this slightly underestimates the quark contribution. The true correction must be less than the 1.1% charge-induced difference between each $e^\pm$ and $\nu\bar{\nu}$ helicity state [13].

Substituting in the values from Table I and expressing T in GeV, Eq. (7) becomes

$$f(T)=1.569+0.569\left[\exp\left[\frac{-0.0234}{T}\right]+6\exp\left[\frac{-0.066}{T}\right]+3\exp\left[\frac{-0.11}{T}\right]+\exp\left[\frac{-0.394}{T}\right]\right.$$
$$\left.+3\exp\left[\frac{-0.413}{T}\right]+3\exp\left[\frac{-1.17}{T}\right]+3\exp\left[\frac{-22}{T}\right]\right]+0.963\exp\left[\frac{-0.10}{T}\right], \tag{9}$$

TABLE I. The values of $\beta_j M_j$ and $T_j M_j$ (as introduced in Sec. III) corresponding to particle rest masses. [The top quark has not yet been observed but must have a mass ≥ 89 GeV (at the 95% C.L.).]

Particle	m_j (GeV)	$\beta_j M_j$ (g)	T_j/β_i (GeV)
Muon	$m_\mu=0.106$	4.53×10^{14}	0.0234
u,d quark	$m_{u,d}\simeq 0.34$	1.60×10^{14}	0.066
s quark	$m_s\simeq 0.5$	9.6×10^{13}	0.11
gluon	$m_g\simeq 0.6$	1.1×10^{14}	0.10
τ	$m_\tau=1.78$	2.68×10^{13}	0.394
c quark	$m_c\simeq 1.87$	2.56×10^{13}	0.413
b quark	$m_b\simeq 5.28$	9.07×10^{12}	1.17
t quark*	$m_t\simeq 100$	0.48×10^{12}	22
Neutral pion	$m_{\pi^0}=0.135$	2.08×10^{14}	0.051
Charged pion	$m_{\pi^\pm}=0.140$	2.01×10^{14}	0.053

for 3 color degrees of freedom. If pions are directly emitted when the power peaks below about Λ_{QH}, and quarks and gluons are directly emitted above Λ_{QH}, Eq. (9) applies for $T \gtrsim \Lambda_{QH}/\beta_{s=1/2} \simeq 0.05-0.06$ GeV and for $T \lesssim \Lambda_{QH}/\beta_{s=1/2}$, we have

$$f(T)=1.569+0.569\exp\left[\frac{-0.0234}{T}\right] +0.267\left[\exp\left[\frac{-0.051}{T}\right]+2\exp\left[\frac{-0.053}{T}\right]\right]. \tag{10}$$

We take $\Lambda_{QH}/\beta_{s=1/2}$, rather than $\Lambda_{QH}/\beta_{s=0}$, to define the transition between these two formulas since the q_u and q_d contribution to $f(T)$ is almost three times the pion contribution.

If a hole can emit three lepton families, six quark flavors, the photon, and direct pions when relevant, then $f(M) \lesssim 13.9$. Extrapolation to peak energies above 100 GeV depends on the particle model. In the Glashow-Weinberg-Salam model [21] there are three fermionic families, the $s=0$ Higgs doublet, the $s=1$ $W^{\pm}$ and Z^0 bosons (Ref. [22]) [$m_W=80.6(\pm 0.4)$ GeV and $m_Z=91.16(\pm 0.03)$ GeV] and no graviton. At nonrelativistic energies, $W^{\pm}$ has a longitudinally polarized state and two transverse polarizations, giving a total of 6 degrees of freedom. At these energies, the longitudinal state absorbs the two Higgs-field degrees of freedom (H^+,H^-) and the Z^0 absorbs one of the H^0 Higgs-boson states. Above the symmetry-breaking scale of the Higgs field, the $W^{\pm}$ longitudinal degree of freedom disappears and the $s=0$ H^+ and H^-, as well as the two H^0 states, appear as real particles. Thus at energies around m_W, there is one $s=0$ mode, 90 $s=1/2$ modes, and 27 $s=1$ modes. At higher energies, there are 4 $s=0$ modes, 90 $s=1/2$ modes and 24 $s=1$ modes. Hence $f(M) \lesssim 15.4$ for peak energies less than about 100 GeV.

Embedding the Glashow-Weinberg-Salam group $U(1)\times SU(2)_L \times SU(3)$ in SU(5), we would have (Ref. [23]) 30 $s=1/2$ modes per family, 4 $s=0$ Weinberg-Salam Higgs modes, 18 further Higgs modes arising from the embedding, 16 $s=1$ gluon modes, $4W^{\pm}$ and $2Z^0$ modes, 2 $s=1$ photon polarizations, and 36 X and Y boson modes (24 of which are $s=1$ and 12 of which are $s=0$). This totals 34 $s=0$ modes, 30 $s=1/2$ modes per family and 48 $s=1$ modes and so, for three fermionic families, $f(M) \lesssim 24.8$ (if we disregard mode mixing). The minimal SU(5) model has no particles with masses between the 300 GeV scale of $SU(2)_L$-symmetry breaking and the 10^{15} GeV scale of SU(5)-symmetry breaking. Other models, such as SO(10), may have intermediate-mass scales which depend on the details of symmetry breaking.

In the $N=1$ supersymmetry model, each $s=1$ particle has an $s=1/2$ superpartner, each $s=1/2$ particle has an $s=0$ superpartner and each $s=2$ particle has an $s=3/2$ superpartner. In this case, $f(M) \lesssim 45$. Theoretical considerations suggest that the rest masses of the $s=0$ superparticles, the major contributors to this bound, are of order 10^3 GeV. The Mark II, ALEPH, and OPAL experiments [54] constrain the masses of any charged $s=0$ superparticles to be greater than about 10 GeV and the Higgs-boson mass is generally expected to be in the range $10-10^3$ GeV. If the photino is the lightest superparticle and has a cosmological density of $\Omega h^2 \lesssim 1$, the photino mass must be [25] greater than about 0.5 GeV. If photino annihilations contribute significantly to the cosmic-ray $\bar{p}$ spectrum, the gravitino mass lies [26] above about 3 GeV. Further species also appear in superstring models. For example, in $E_8 \times E_{8'}$ superstring models [27], the particles in our E_8 world are complemented by "shadow" particles in the other $E_{8'}$ sector. These only interact gravitationally with "our world." The black-hole emission rates above a few GeV are then doubled and the lifetimes halved [28]. If the symmetry breaking is different for the shadow matter, so that the shadow particles remain massless at very low energies, the emission rates below 1 GeV may increase by orders of magnitude. This would substantially decrease the black-hole lifetime and hence increase M_*, the mass of a hole whose lifetime equals the present age of the Universe.

In alternative theories, the Higgs, W, Z bosons and perhaps leptons and quarks may be composed of more fundamental particle (e.g., preons [29], technifermions [30], leptoquarks [31]), on scales of order 10^3 GeV or above. Novel interactions above the Fermi mass, 3.54×10^2 GeV, may exist. The number of degrees of freedom or subparticles is strongly model dependent. In some theories, notably the Dimopoulos technicolor model [32], further composite states (for example, a large number of pseudo Goldstone bosons) appear before the deconfinement scale is reached. As a rough estimate, we expect the number of new subparticle modes in these theories to be $\sim 10^2$, comparable with the number introduced in supersymmetric models. This would give $f(M) \lesssim 10^2$.

In summary, measurement of the instantaneous emission rate from a high-temperature black hole should give us information on the correct particle model at high energies. However, any present distribution of holes created in the early Universe is only appreciably modified if there exist further low mass ($\mu \lesssim 0.3$ GeV) or massless particle modes which couple to the $10^{14}-10^{15}$ g holes, thereby decreasing their lifetime. In this case, the present number density of PBH's would peak at a higher mass [15].

IV. THE BLACK-HOLE LIFETIME

Integrating Eq. (5), we obtain the black-hole lifetime

$$\tau_{\rm evap}=1.87\times 10^{-27}\int_{M_{\rm min}}^{M_i}\frac{M^2}{f(M)}dM \text{ sec} =1.19\times 10^3\frac{G^2M_i^3}{\hbar c^4 f_L(M_i)}, \tag{11}$$

where M_i is the initial mass of the hole in g and $f_L(M_i)^{-1}$ is the mass-squared average of $f(M)^{-1}$ over the lifetime. $M_{\rm min}$, the mass at which Eq. (1) breaks down, is strictly greater than about the Planck mass. Because $f(M)^{-1}$ varies weakly compared with M^2, the life-

time is approximately

$$\tau_{\rm evap} \simeq 1.19\times10^{3}-\frac{G^2M_i^3}{\hbar c^4 f(M_i)} = \begin{cases} 6.24\times10^{-27}M_i^3 f(M_i)^{-1} \text{ sec}, \\ 1.98\times10^{-34}M_i^3 f(M_i)^{-1} \text{ yr} . \end{cases} \quad (12)$$

An $M_i=10^{13}$ g hole [$f(M_i)\simeq 12.5$], initially emitting quarks and gluons, evaporates in about 1.58×10^4 yr; an $M_i=4\times10^{11}$ g hole [$f(M_i)\simeq 15$] evaporates in about 1 yr; and an $M_\odot\simeq 2\times10^{33}$ g hole [$f(M_i)=1$] evaporates in about 10^{66} yr. Since $\tau_{\rm evap}\propto M_i^a$, a hole spends most of its life close to its initial temperature. Primordial holes evaporating today only emit quarks and heavier particles in the final stages, when M reaches 1.8×10^{14} g. This phase lasts 2×10^8 yr less than 1/60 the lifetime of an M_* hole.

We can now calculate more accurately estimates [7,12] of M_*, the mass of a hole whose lifetime equals t_u, the present age of the Universe. An M_* hole, initially emitting $e^\pm$, γ, and $\nu\bar{\nu}$, is close to the thresholds for $\mu^\pm,\pi^{\pm,0}$ and quark emission. To include the latter contributions, we take Page's and Simkin's numerically calculated power [33] as a function of $M_i\mu$. Since we must solve Eq. (12) for M_i, and $f(M_i)$ cannot be expressed simply as an analytic function of M_i, we estimate a value for M_i, calculate $f(M_i)$ and then further refine our M_i estimate. The age of a Friedmann universe with curvature k, present total cosmological matter density Ω_m and Hubble constant $H_0=100h$ km sec^{-1} Mpc^{-1} is

$$t_u = \begin{cases} h^{-1}[(1-\Omega_m)^{-1}-0.5\Omega_m(1-\Omega_m)^{-3/2}\text{arccosh}(2\Omega_m^{-1}-1)], & k=-1,\Omega_m<1 , \\ 2H_0^{-1}/3=6.45\times10^9 h^{-1}\text{ yr}, & k=0,\Omega_m=1.0 . \end{cases} \quad (13)$$

For an $\Omega_m=0.06$ (baryon-dominated) universe, we have $t_u=8.97\times10^9 h^{-1}$ yr. Assuming that the holes take a negligible time to form in the early Universe, Eq. (12) becomes

$$M_* \simeq \begin{cases} 3.56\times10^{14} f(M_*)^{1/3}h^{-1/3}\text{ g}, & \Omega_m=0.06 , \\ 3.19\times10^{14} f(M_*)^{1/3}h^{-1/3}\text{ g}, & \Omega_m=1.0 . \end{cases} \quad (14)$$

As an illustration, Eq. (14) is solved by $f(M_*)=1.933$ and $M_*=4.30\times10^{14}$ g if $h=0.8$ and $\Omega_m=1.0$. In this case, the muon contribution is $f_\mu(M_*)=0.255$, the pion contribution is $f_\pi(M_*)=0.104$ (for an average pion mass of 0.138 GeV) and the q_u and q_d contribution is less than 10^{-2}. Figure 1 shows M_* as a function of h for $\Omega_m=0.06$ and $\Omega_m=1.0$, so derived. M_* falls in the range

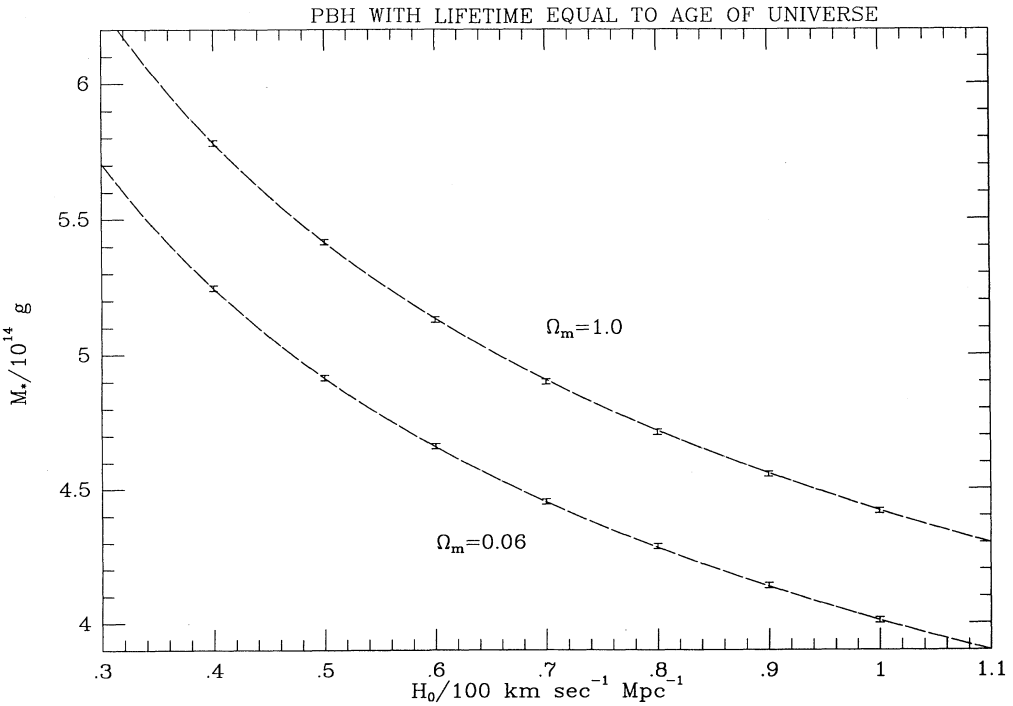

FIG. 1. The mass of a primordial black hole just expiring today, M_*, as a function of the Hubble parameter $h=H_0/(100\text{ km sec}^{-1}\text{ Mpc}^{-1})$, for $\Omega_m=0.06$ and $\Omega_m=1.0$.

$$5.78(\pm0.01)\times10^{14}\ \text{g}\gtrsim M_*\gtrsim 4.42(\pm0.01)10^{14}\ \text{g}\ ,\quad \Omega_m=0.06\ ,$$
$$5.25(\pm0.01)\times10^{14}\ \text{g}\gtrsim M_*\gtrsim 4.01(\pm0.01)10^{14}\ \text{g}\ ,\quad \Omega_m=1.0\ , \tag{15}$$

for $0.4\le h\le 1.0$. To good accuracy, we can parametrize the curves by

$$M_*\simeq\begin{cases}4.42(\pm0.01)\times10^{14}h^{-0.293\pm0.003}\ \text{g}\ , & \Omega_m=0.06\ ,\\ 4.01(\pm0.01)\times10^{14}h^{-0.293\pm0.002}\ \text{g}\ , & \Omega_m=1.0\ .\end{cases} \tag{16}$$

M_* would be proportional to $h^{-1/3}$ if τ_{evap} were independent of $f(M_*)$. t_u must also be consistent with the independent nucleo-cosmochronology estimates [34] of the age of the Galaxy, $\tau_G\simeq 9.5-21\times10^9$ yr. This implies that $h\lesssim 0.944$ for $\Omega_m\ge 0.06$ or $h\lesssim 0.679$ for $\Omega_m=1.0$ and, for all Ω_m, $M_*\ge 4.49(\pm0.01)\times10^{14}$ g.

Equations (15) and (16) substantially improve Page's best estimate [12]: $M_*\simeq 5(\pm1)\times10^{14}$ g for $t_u=8-18\times10^9$ yr and only two neutrino species. We have used an average pion mass, though, since only the π^0 emission rates were available [18]. This slightly underestimates (overestimates) the π^0 ($\pi^\pm$) contribution but only produces a net change in $f(M_i)$ of order 0.1%. Electric charge also slightly decreases the $\pi^\pm$ emission rate. On the other hand, Eq. (12) assumes that $f_L(M_i)=f(M_i)$. This means that M_*, and hence $f_L(M_*)$, are somewhat underestimated since they do not include the emission at smaller M. More importantly, there is the uncertainty in the $\pi^{\pm,0}$ and $q_{u,d}$ production around Λ_{QH}. If no pions are emitted below 300 MeV and $q_{u,d}$ are emitted above 300 MeV, we find that $M_*\simeq 5.28\times10^{14}$ g for $\Omega_m=0.06$ and $h=0.53$. Alternatively if pions are directly emitted below 300 MeV, then $M_*\simeq 5.32\times10^{14}$ g. This is a change of less than 1%. Since some pions should be directly emitted at low energies, this represents the maximal possible error in Eq. (16) due to the uncertainties around Λ_{QH}. The further refinement of integrating Eq. (11) for each $f(M_*)$ and M_* estimate, using Page's nonrelativistic tables, is not justified. Including massless gravitons increases M_* by less than 1%. Because $f_L(M_i)^{-1}$ is the mass-squared lifetime average of $f(M_i)^{-1}$, any new phenomena above 100 GeV can have little effect on M_*: 10^7-10^8 new $s=1/2$ modes would be needed at 100 GeV to increase M_* by 1%. M_* can only be significantly affected if further species with small spin and $\mu\lesssim 0.3$ GeV exist.

In our simulations of the lifetime emission, it was not practical to program Page's tabulated power versus $M\mu$ into the computer. Hence to calculate the time when particles are emitted and their present redshifted energy, we used an approximation for $f_L(M_i)$ which is weighted by the $T>T(M_i)$ emission. We assumed that each species j increases $f(M)$ stepwise by the relativistic contribution f_j as M reaches $\beta_j M_j$ [cf. Eq. (7)], so that

$$\tau_{\text{evap}}\simeq 3.58\times10^3\frac{G^2}{\hbar c^4}\left[\int_{\beta_1M_1}^{M_i}\frac{M^2}{f(M_i)}dM+\int_{\beta_2M_2}^{\beta_1M_1}\frac{M^2}{f(M_i)+f_1}dM+\int_{\beta_3M_3}^{\beta_2M_2}\frac{M^2}{f(M_i)+f_1+f_2}dM+\cdots+\int_0^{\beta_nM_n}\frac{M^2}{f(M_i)+\sum_{j=1}^{n}f_j}dM\right] \tag{17}$$

and

$$f_L(M_i)\simeq\left[\frac{1}{f(M_i)}-\frac{f_1(\beta_1M_1/M_i)^3}{f(M_i)[f(M_i)+f_1]}-\frac{f_2(\beta_2M_2/M_i)^3}{[f(M_i)+f_1][f(M_i)+f_1+f_2]}-\cdots\right]^{-1}. \tag{18}$$

Equation (18) is displayed to two terms in Fig. 2. The greatest discontinuity occurs as quarks are introduced. Equation (18) neglects the decrease in j emission at $M\simeq\beta_jM_j$. It also neglects the constraint that the total energy of an emitted particle is greater than its rest mass. On the other hand, the high-energy tail in Eq. (1) implies that some j particles are emitted before M reaches β_jM_j. Since the distribution falls off less steeply at high energies than it rises at low energies, these corrections roughly cancel.

V. EMISSION OVER LIFETIME

Neglecting redshift for the moment, the total distribution of particles emitted by black hole over its lifetime is

$$\frac{dN}{dQ}=\int_{T(M_i)}^{T(M_{\min})}\frac{d\dot N}{dQ}\left[\frac{dt}{dM}\frac{dM}{dT}\right]dT\ . \tag{19}$$

Using Eqs. (2) and (5) and including decays, the number spectrum for species X becomes

$$\frac{dN_X}{dE}=3.59\times10^{-2}\frac{\hbar c^5}{Gk^3}\int_{T(M_i)}^{T(M_{\min})}f(T)^{-1}T^{-4}\sum_j\int_{Q=E}^{Q=\infty}\frac{\Gamma_j(Q,T)}{\exp(Q/kT)-(-1)^{2s_j}}\frac{dg_{jX}(Q,E)}{dE}dQ\,dT\ , \tag{20}$$

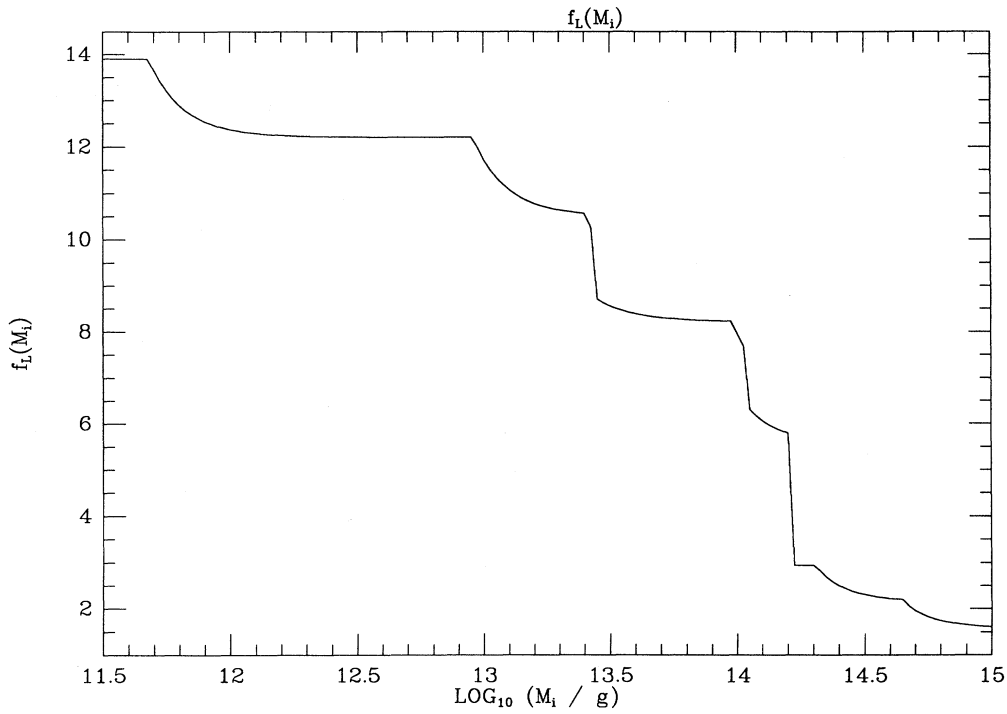

FIG. 2. The approximation for $f_L(M_i)$ given in Eq. (18) as a function of initial black-hole mass M_i.

where the sum is over all parent species j and degrees of freedom. As we show in Sec. VI, Eq. (20) implies that $dN/dE \propto E^{-3}$ for $E \gg T(M_i)$. Prior to decay, the $T \simeq T(M_i)$ emission should dominate $E \lesssim T(M_i)$. Since dg_{jX}/dE degrades the emission into less energetic particles, decays should further enhance the low-energy flux. From Eq. (10) in Ref. [10] and Eq. (5) above, the number of particles emitted over the lifetime per nondecaying $s=1/2$ state is

$$N_{s=1/2}=\int_{M_{\min}}^{M_i}\frac{dN}{dt}\frac{dt}{dM}dM \simeq 10^9 M_i^2 f(M_i)^{-1} \tag{21}$$

if M_i is in g. For 10^2 directly emitted states, $N_d \simeq 10^{10}-10^{11}M_i^2$. Regardless of whether the emission decays, the hole releases a total energy of

$$E_{\text{tot}}=M_i c^2=5.61\times 10^{23} M_i \text{ GeV} \tag{22}$$

over its lifetime.

VI. ANALYTIC APPROXIMATIONS TO EMISSION SPECTRA

Let $dg_{jh}(Q,E)/d\ln E$ describe the decay of particle j with energy Q into a hadron h which is stable on beam-collider time scales. One can show that a good approximation to the QCD jet fragmentation function is [10]

$$\frac{dg_{jh}}{dE}=\frac{G}{E}\left[1-\frac{E}{Q}\right]^{2m-1}\Theta(E-km_hc^2) \tag{23}$$

for general Q. In Eq. (23), Θ is the Heaviside function, $km_hc^2=O(m_hc^2)$ is the energy at the function's peak, $m=1$ (2) if h is a meson (baryon) and G is a normalizing constant which depends on j and h. [Strictly Eq. (23) is only valid in the relativistic limit.] The peak energy is almost stationary as a function of Q for $\pi^{\pm}$ and increases slightly for $p\bar{p}$. We combine Eqs. (23) and (3), recall that $\Gamma_j \propto Q^2T^{-2}$ for relativistic or $s=1/2$ particles and put $Y=Q/kT$. The emitted spectrum of h particles, integrated over the lifetime of a hole at constant redshift, is then approximately

$$\frac{dN_h}{dE}\propto E^{-1}\int_{T(M_i)}^{T_{pl}}\int_{E/T}^{\infty}\frac{Y^2T^{-3}(1-E/YT)^{2m-1}}{\exp(Y)-(-1)^{2s_j}}\times\Theta(E-km_hc^2)dY\,dT\ . \tag{24}$$

(i) For $E \simeq km_hc^2 \lesssim T(M_i)$, the major contribution to the lifetime emission comes from the lower bounds of the integrals and the spectra should resemble the low-Q fragmentation functions.

(ii) For $E \gtrsim T(M_i), Q \simeq T(M_i)$ dominates. The behavior is determined by the instantaneous $T(M_i)$ emission (see Ref. [10]) and so $dN_h/dE \propto E^{-1}$.

(iii) For $E \gg T(M_i)$, the temperature distribution T^{-3} falls off less steeply than the high-energy exponent cutoff at fixed T and the $T \simeq E$ contribution gives $dN_h/dE \propto E^{-3}$.

In the jets, half the protons and/or antiprotons are final cluster states (on collider time scales) and half are

neutron β decays. Since the $p\bar{p}$ are generally products of fewer decay steps and reasonably heavy hadrons (thus suffering less momentum smearing in the decays), the above discussion should apply most strongly to them.

If j is a nondecaying primary species, we have $dg_{jX}/dE=\delta(Q-E)$ and so

$$\frac{dN_d}{dE} \propto \int_{T(M_i)}^{T_{pl}} \Gamma_j(E,T)T^{-4} \times[\exp(E/T)-(-1)^{2s_j}]^{-1}dT \ . \quad (25)$$

(i) For $E \ll T(M_i)$, the low-energy form of $d\dot{N}/dE$ (see

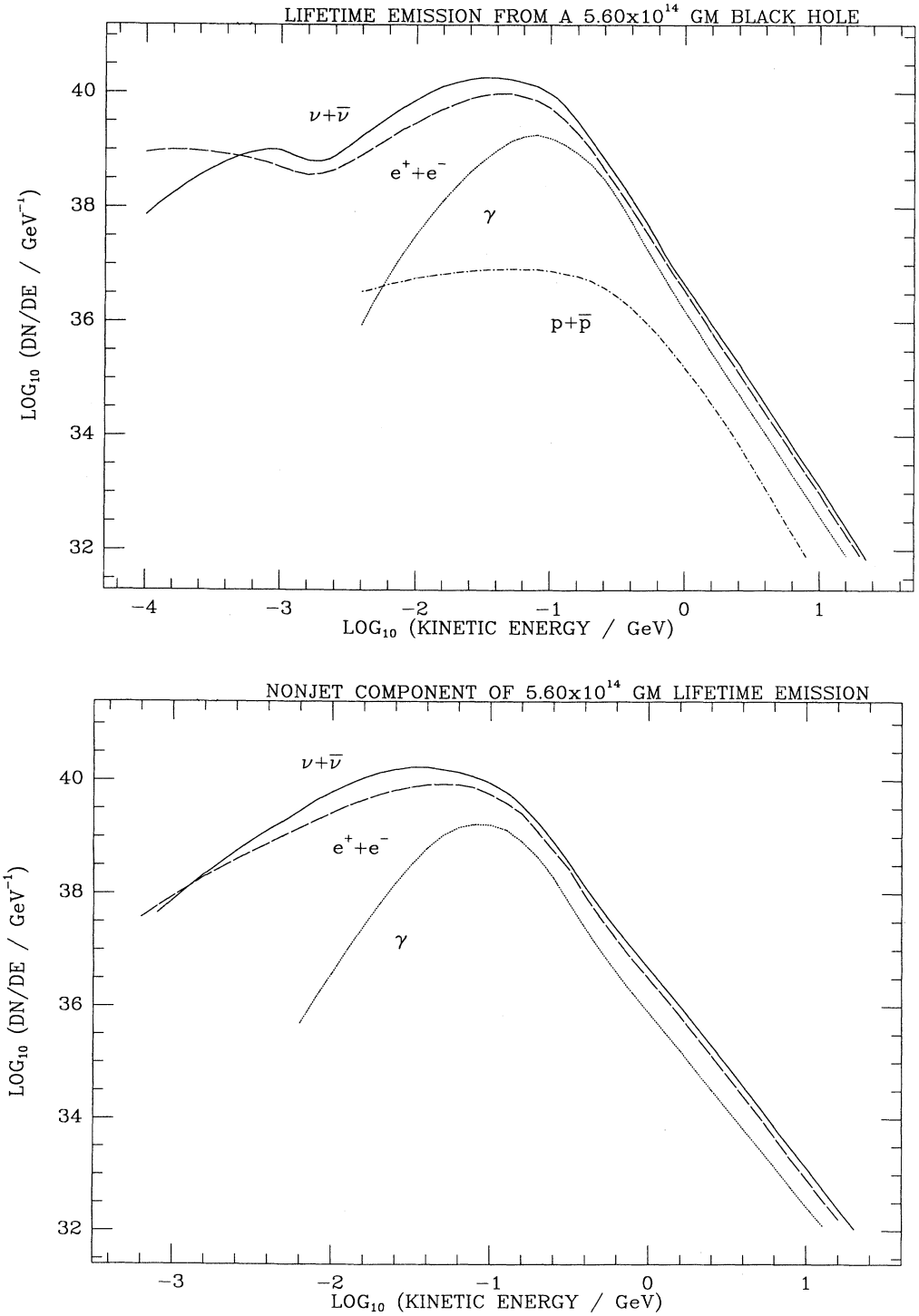

FIG. 3. (a) The unredshifted lifetime emission from an $M_i=5.60\times10^{14}$ g black hole. (b) The nonjet component of the emission.

Ref. [10]) implies that

$$\frac{dN_d}{dE} \propto \begin{cases} E^1, & s_j=0 \ , \\ E^2, & s_j=1/2 \ , \\ E^3, & s_j=1 \ . \end{cases} \tag{26}$$

(ii) For $E \gtrsim T(M_i)$, Eq. (25) becomes

$$\frac{dN_d}{dE} \propto E^{-3} \int_{E/T_{pl}}^{E/T(M_i)} Y^4 [\exp(Y) - (-1)^{2s_j}]^{-1} dY$$
$$\propto E^{-3} \ . \tag{27}$$

Electrons, positrons, photons, and neutrinos are both directly emitted and created in jets. The primary nondecaying emission should produce bumps on these spectra at $E \gtrsim T(M_i)$, between the E^{-1} and E^{-3} slopes, provided that $T(M_i) \gtrsim 100$ MeV. At lower initial temperatures, the nonjet emission becomes the major contributor at all energies.

VII. NUMERICAL SIMULATION OF THE EMISSION

Our method of simulating the emission follows that described in Ref. [10]. We convolve Eq. (20) with the Monte Carlo jet code BIGWIG [35,36] written for collider events. The temperature is chosen by randomly generating $Y=T^{-2} \in (Y(T_{\max}), Y(T_{\min}))$. The particle species is taken from the list $\nu\bar{\nu}$, γ, $e^{\pm}$, $\mu^{\pm}$, $\tau^{\pm}$, gluon, quark or, if pions are directly emitted and $T<0.07$ GeV, $\pi^{\pm}$ or π^0. [The primary $s=1/2$ flux from a $T=0.07$ GeV hole peaks at $m_{u,d} \simeq 0.30$ GeV. Ideally, pions should be directly emitted if $Q \lesssim 0.30$ GeV. This, however, is extremely difficult to program since the Q distribution in Eq. (1) depends on s.] If there are no primary pions, we save time by only generating $\tau^{\pm}$, quarks or gluons if $T \geq 0.3/X_{\max}$ GeV where $X_{\max}$ is the maximum allowed value of Q/T. In all cases, the particle is weighted by its degrees of freedom; the relative flux of that species per degree; and $f(T)^{-1}$ [using the approximation of Eq. (10)]. BIGWIG then decays the particle, keeping rest masses to the nearest MeV. The results are histogrammed using the CERN library HBOOK. Typically, the program creates $n \simeq 45\,000$ (unweighted) initial particles using $M_i \simeq 10^{14}$ g, $X_{\max}=8.5-10$ and $T_{\max}=30$ GeV. Since $dN/dT \propto T^{-2}$, varying $T_{\max}$ around this value has little effect on our lifetime spectra, as we confirm in Sec. VIII D. In one version, we redshift the emission from an M_* hole which formed in the early universe. The time at emission is the difference between t_u and the lifetime of a hole with initial temperature T, applying the approximation Eq. (17). We then solve the redshift equations [14] for a Friedmann universe with values of Ω_m and H_0 which correspond to M_*.

The spectra are normalized by noting that the total unredshifted energy is $E_{\text{tot}}=M_i c^2$. The maxima of the $dN_{\nu\bar{\nu}}/dE$ and $\log_{10}(dN_{\nu\bar{\nu}}/dE)$ vs $\log_{10}E$ histograms are next matched. The estimated error in this normalization method is less than 10% for $n \simeq (2-10)\times 10^5$ initial particles. We chose this approach, rather than a purely numerical one, to minimize the total statistical error. An upper estimate of any systematic error in calculating

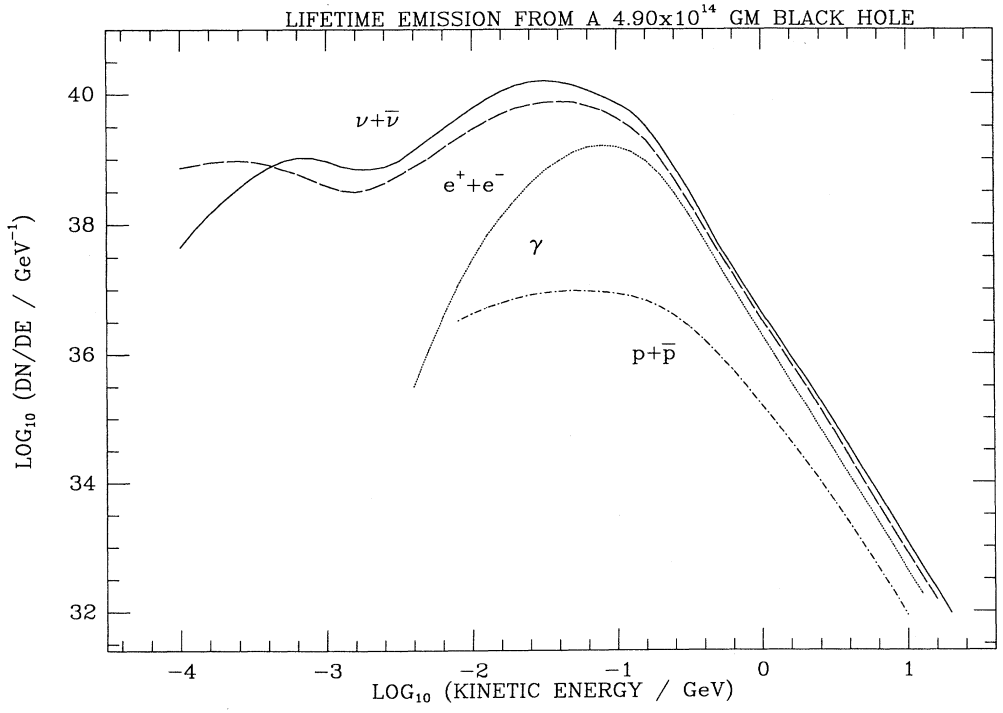

FIG. 4. The unredshifted lifetime emission from an $M_i=4.90\times 10^{14}$ g black hole.

TABLE II. The errors in plotting $\log_{10}(dN/dE)$ as a function of energy $\log_{10}E$ in Figs. 3–7. The errors at all other energies are less than 10%.

Figure	$p\bar{p}$	$e^{\pm}$	γ	$\nu\bar{\nu}$
3(a)	30% at $E<25$ MeV 50% at $E>2$ GeV	30% at $E<1$ MeV 30% at $E>6$ GeV	30% at $E<25$ MeV 30% at $E>3$ GeV	30% at $E<3$ MeV 30% at $E>3$ GeV
3(b)		30% at $E<3$ MeV 50% at $E>3$ GeV	30% at $E<25$ MeV 50% at $E>3$ GeV	30% at $E<2$ Mev 30% at $E>3$ GeV
4	30% at $E<25$ MeV 30% at $E>3$ GeV	30% at $E<1$ MeV 20% at $E>3$ GeV	30% at $E<25$ MeV 20% at $E>3$ GeV	30% at $E<1$ MeV 20% at $E>3$ GeV
5	50% all E	20% at $E<1$ MeV 50% at $E>3$ GeV	30% at $E<5$ MeV 50% at $E>3$ GeV	50% at $E<3$ MeV 50% at $E>3$ GeV
6	40% all E	30% at $E<1.6$ MeV 50% at $E>3$ GeV	30% at $E<25$ MeV 50% at $E>3$ GeV	50% at $E<1.6$ MeV 50% at $E>3$ GeV
7	30% at $E<50$ MeV 50% at $E>6$ GeV	30% at $E<1$ MeV 30% at $E>10$ GeV	30% at $E<25$ MeV 50% at $E>10$ GeV	30% at $E<1$ MeV 30% at $E>10$ GeV

dN/dE is 10%, except at high $x=p/Q$ where the statistical errors are comparable with any systematic error. (Here p is particle momentum.) The systematic error is much less than 10% around the distribution peaks [35]. Although tightly constrained, BIGWIG gives a good account of the existing e^+e^- annihilation data for initial quark or gluon energies of 1.8–20 GeV. At low Q, experimental data is scarce. In our simulations, we neglect the changes in Γ_s due to particle charge and nonrelativistic emission. This is justified for the primary $e^{\pm}$ and $\nu\bar{\nu}$ since the nonrelativistic corrections apply at most to a tiny fraction of the spectrum. More importantly, the $M \lesssim M_*$ holes are starting to emit hadrons or their constituents. These particles with their huge increase in internal degrees of freedom dominate the primary leptons. As we mentioned earlier, the uncertainty in hadron

TABLE III. Final states, total energy, spectra peaks, average multiplicities, and average kinetic energies for the lifetime emission of an $M_i=5.60\times10^{14}$ g hole.

$M_i=5.60\times10^{14}$ g	$p\bar{p}$	$e^{\pm}$	γ	$\nu\bar{\nu}$
Number	$2.28(\pm0.18)\times10^{36}$	$9.49(\pm0.19)\times10^{38}$	$2.55(\pm0.07)\times10^{38}$	$1.79(\pm0.04)\times10^{39}$
Number (% of $N_{\rm tot}$)	0.08% (±0.005%)	31.70% (±0.16%)	8.52% (±0.09%)	59.71% (±0.25%)
		$N_{\rm tot}=2.99(\pm0.05)\times10^{39}$		
Jet products (% of $N_{\rm tot}$)	0.08% (±0.05%)	2.36% (±0.31%)	2.72% (±0.17%)	6.95% (±0.48%)
$\left.\frac{dN}{dE}\right\|_{\rm peak}$ (GeV^{-1})	$8.2(\pm0.4)\times10^{36}$	$7.5(\pm0.4)\times10^{39}$	$1.8(\pm0.1)\times10^{39}$	$1.75(\pm0.1)\times10^{40}$
at $E_{\rm peak}$(GeV)	0.070 (±0.015)	0.038 (±0.005)	0.071 (±0.010)	0.031 (±0.005)
Net energy (GeV)	$2.78(\pm0.22)\times10^{36}$	$1.00(\pm0.02)\times10^{38}$	$3.98(\pm0.11)\times10^{37}$	$1.73(\pm0.04)\times10^{38}$
Energy (% of $E_{\rm tot}$)	0.88% (±0.07%)	31.75% (±0.79%)	12.61% (±0.35%)	54.75% (±1.37%)
		$E_{\rm tot}=3.14\times10^{38}$ GeV		
Jet products (% of $E_{\rm tot}$)	0.88% (±0.07%)	2.6% (±1.5%)	5.22% (±0.58%)	7.17% (±2.6%)
Multiplicities	0.001 (±0.001)	0.515 (±0.001)	0.140 (±0.001)	0.969 (±0.002)
$\bar{E}$ (GeV)	0.283 (±0.006)	0.104 (±0.001)	0.156 (±0.001)	0.097 (±0.001)

production around Λ_{QH} is at least comparable with the nonrelativistic corrections to Γ_s.

VIII. THE RESULTS

The lifetime particle-plus-antiparticle emissions are displayed in Figs. 3, 4, and 7 for case (i) $M_i = 5.60\times10^{14}$ g; case (ii) $M_i = 4.90\times10^{14}$ g; and case (iii) $M_i = 7.00\times10^{13}$ g. These correspond to initial temperatures of $T(M_i)=0.019$, 0.021, and 0.151 GeV, respectively. The lifetime of the hole equals t_u in case (i) if $\Omega_m = 1$ and $H_0 = 32$ km sec^{-1} Mpc^{-1}; in case (ii) if $\Omega_m = 0.06$ and $H_0 = 70$ km sec^{-1} Mpc^{-1}; and in case (iii), $\tau_{evap} \simeq 8\times10^6$ yr. Initially we neglect the cosmological redshift, or equivalently assume that evaporation occurs in the present era. This is done to remain independent of the cosmological model, the epoch of evaporation and any assumptions concerning the initial distribution of black holes. The maximum errors in plotting the spectra are presented in Table II. Since BIGWIG stores rest masses to 1 MeV, the spectra may be unreliable below 1 MeV. However, most low-energy photons in all cases, and most low-energy $e^{\pm}$ and $\nu\bar{\nu}$ in cases (i) and (ii), are nondecaying primary emission which BIGWIG treats exactly. The $W^{\pm}$ and Z^0 emission is not included. These bosons, which are only emitted in significant numbers above $T \simeq 15$ GeV, have little effect on the lifetime spectra. The emission of q_t, weak bosons and hypothetical particles is discussed in Ref. [10].

A. $M_i \simeq M_*$ emission

The shape of the spectra agrees well with our analytic discussion in Sec. VI. It differs little between cases (i) and (ii). The hole evaporates for most of its life around its initial temperature. Below $E \simeq 0.2$ GeV, dN/dE strongly resembles the instantaneous emission from a $T \simeq 0.02$–0.1 GeV black hole [10], together with a small jet-produced $n\bar{n}$ and $p\bar{p}$ contribution from higher temperatures. The spectra peak at $E \simeq 0.02$–0.2 GeV and fall off with an E^{-3} slope above $E \simeq 0.2$ GeV. dN/dE_γ has an E^3 slope between $0.003 \lesssim E \lesssim 0.03$ GeV from the primary photons. $dN/dE_{e^{\pm},\nu\bar{\nu}}$ has a slope of about E^2 between $0.003 \lesssim E \lesssim 0.03$ GeV from the primary $\mu^{\pm}$ and $\pi^{\pm}$ decays and the primary $e^{\pm}$ and $\nu\bar{\nu}$ emission, and a small peak below $E \simeq 0.003$ GeV from jet neutron β decay. The main contributor to $dN/dE_{e^{\pm},\gamma,\nu\bar{\nu}}$ at all energies is the $M \simeq M_i$ nonjet emission. At high energies, there is a significant jet contribution (as evidenced by the $p\bar{p}$ tail) and a smaller $\pi^{\pm,0}$ and $\mu^{\pm}$ contribution [Figure 3(b) shows for comparison the nonjet component in case (i).] $dN/dE_{p\bar{p}}$, which is solely jet produced, falls off less quickly at high E than the other spectra—not only are more $p\bar{p}$ produced as T increases, but the instantaneous $p\bar{p}$ flux cuts off less steeply at fixed T than for other species [10]. The energies at which $dN/dE_{e^{\pm},\gamma,\nu\bar{\nu}}$ peaks differ between cases (i) and (ii) by less than the statistical errors (see Tables III and IV). The $dN/dE_{p\bar{p}}$ peaks are

TABLE IV. Final states, total energy, spectra peaks, average multiplicities, and average kinetic energies for the lifetime emission of an $M_i = 4.90\times10^{14}$ g hole.

$M_i = 4.90\times10^{14}$ g	$p\bar{p}$	$e^{\pm}$	γ	$\nu\bar{\nu}$
Number	$2.28(\pm0.16)\times10^{36}$	$7.67(\pm0.15)\times10^{38}$	$2.28(\pm0.06)\times10^{38}$	$1.49(\pm0.03)\times10^{39}$
Number (% of N_{tot})	0.09% (±0.005%)	30.86% (±0.15%)	9.18% (±0.09%)	59.87% (±0.25%)
		$N_{tot} = 2.49(\pm0.04)\times10^{39}$		
Jet products (% of N_{tot})	0.09% (±0.005%)	2.82% (±0.29%)	3.30% (±0.17%)	8.31% (±0.46%)
$\left.\frac{dN}{dE}\right\|_{peak}$ (GeV^{-1})	$6.8(\pm0.3)\times10^{36}$	$5.9(\pm0.3)\times10^{39}$	$1.6(\pm0.1)\times10^{39}$	$1.5(\pm0.1)\times10^{40}$
at E_{peak} (GeV)	0.070 (±0.015)	0.038 (±0.005)	0.071 (±0.010)	0.031 (±0.005)
Net energy (GeV)	$2.85(\pm0.22)\times10^{36}$	$8.61(\pm0.20)\times10^{37}$	$3.67(\pm0.10)\times10^{37}$	$1.50(\pm0.04)\times10^{38}$
Energy (% of E_{tot})	1.03% (±0.08%)	31.26% (±0.74%)	13.31% (±0.35%)	54.40% (±1.30%)
		$E_{tot} = 2.75\times10^{38}$ GeV		
Jet products (% of E_{tot})	1.03% (±0.08%)	2.97% (±1.42%)	5.95% (±0.57%)	8.1% (±2.0%)
Multiplicities	0.002 (±0.001)	0.540 (±0.001)	0.162 (±0.001)	1.047 (±0.002)
$\bar{E}$ (GeV)	0.314 (±0.010)	0.111 (±0.001)	0.161 (±0.001)	0.101 (±0.001)

associated with low-energy jets while the $dN/dE_{e^{\pm},\gamma,\nu\bar{\nu}}$ peaks are produced by the nonrelativistic primary or low-energy jet pions. As M_i decreases, the number of primary particles emitted over $\tau_{\rm evap}$ decreases and the increase in average particle momentum smears out the decay spectra. Thus the heights of the main peaks and the lepton β decays peaks are 10–30 % smaller in case (ii).

Jet products account for 12.1($\pm$0.8)% of $N_{\rm tot}$ (the total number of final states produced over $\tau_{\rm evap}$) in case (i) and 15.5($\pm$0.8)% in case (ii). About 35% of the photons are jet products (see Tables II and IV). The fractions of $N_{\rm tot}$ in each species differ between (i) and (ii) by of order the statistical errors. Although protons and antiprotons make up about 1.5–2.0 % of the jet-dominated instantaneous $T\simeq 0.3$–100 GeV flux [10], here they make up about 0.1%. This is because most jets have low initial energy and produce few $p\bar{p}$. $N_{\rm tot}$ differs by $\Delta N_{\rm tot}/N_{\rm tot}\simeq 19\%$ between cases (i) and (ii). We can justify this value as follows. From Eq. (21), prior to decay we have $N_{\rm tot}\propto M_i^2$. Noting that $(M_i+\Delta M_i)^2 \simeq M_i^2(1+2\Delta M_i/M_i)$ for $\Delta M_i \ll M_i$, we would then expect that

$$\frac{\Delta N_{\rm tot}}{N_{\rm tot}}\simeq\frac{2\Delta M_i}{M_i}\simeq 26\% \tag{28}$$

for a fixed number of species. This overestimates the true value because the average multiplicities of decay states per primary particle increases as M_i decreases. Since the $p\bar{p}$ are emitted at high temperatures, $N_{p\bar{p}}$ changes little between the two cases. Because the $T>100$ GeV evaporation lasts $10^{-10}\tau_{\rm evap}$, the uncertainties in any particle model at very high energies can also have little effect on $N_{\rm tot}$. The multiplicities, averaged over the lifetime emission, resemble the $T=0.02$ GeV values increased slightly by low-energy jets. The $e^{\pm}$, γ, and $\nu\bar{\nu}$ multiplicities are 5–15 % greater in case (ii) since more of the lifetime is spent emitting quarks and gluons. The $\nu\bar{\nu}$, with the highest multiplicities per jet, increase the greatest.

The unredshifted energy, prior to decay and averaged over the lifetime emission, is 0.171($\pm$0.002) GeV in case (i) and 0.194($\pm$0.002) GeV in case (ii). Noting that [10] the average energy of the primary $s=1/2$ flux is $4.02T$, we could associated these energies with black-hole masses of (i) $\bar{M}=2.49(\pm 0.03)\times 10^{14}$ g and (ii) $\bar{M}=2.19(\pm 0.02)\times 10^{14}$ g, respectively. Such $\bar{M}$ holes would predominantly emit primary $e^{\pm}$, γ, and $\nu\bar{\nu}$, as well as some $\mu^{\pm}$, π^0, $\pi^{\pm}$, and low mass quarks. Jet products carry 15.9 ($\pm$3.9)% of $E_{\rm tot}$ in case (i) and 18.1($\pm$3.1)% in case (ii). The fractions of $E_{\rm tot}$ in each species and the average $e^{\pm}$, γ, and $\nu\bar{\nu}$ kinetic energies resemble those for an $\bar{M}$ hole with a small jet contribution from higher T. The average $p\bar{p}$ energy is associated with low-energy jets. The average energies increase as M_i decreases, not only because the emission starts at a higher temperature, but because the hole spends less of its lifetime around M_i.

B. Redshifted $M_i\simeq M_*$ emission

Figure 5 and Table V display the redshifted emission from an $M_i=5.60\times 10^{14}$ g hole. In this example, the PBH just completes its evaporation today in an $\Omega_m=1.0$, $h=0.32$ Friedmann universe. BIGWIG's rounding off of rest mass is only relevant below redshifted energies of

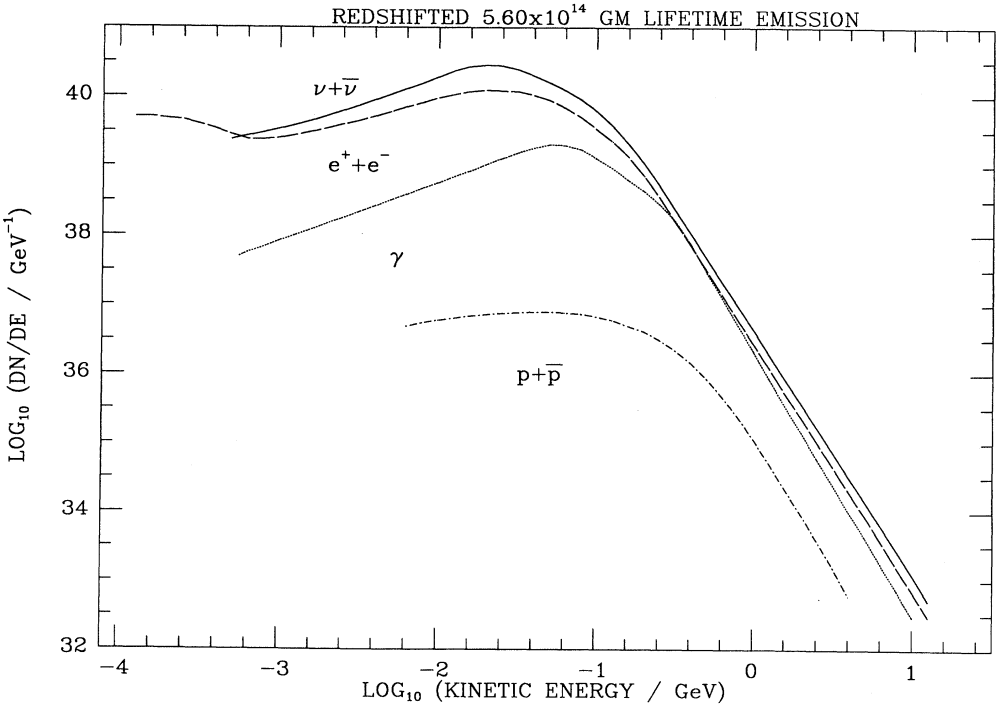

FIG. 5. The redshifted lifetime emission from an $M_i=5.60\times 10^{14}$ g black hole.

TABLE V. Total redshifted energy, spectra peaks, and average redshifted kinetic energies for the lifetime emission of an $M_i = 5.60 \times 10^{14}$ g hole formed in the early universe.

$M_i = 5.60 \times 10^{14}$ g	$p\bar{p}$	$e^{\pm}$	γ	$\nu\bar{\nu}$
Net redshifted energy (GeV)	2.54(±0.42) $\times 10^{36}$	7.34(±0.27) $\times 10^{37}$	3.23(±0.11) $\times 10^{37}$	1.29(±0.05) $\times 10^{38}$
Redshifted energy (% of E_{tot})	1.07% (±0.18%)	30.96% (±1.14%)	13.62% (±0.48%)	54.64% (±1.94%)
		$E_{tot} = 2.37(\pm 0.04) \times 10^{38}$ GeV		
Jet products (% of E_{tot})	1.07% (±0.18%)	3.13% (±2.2%)	6.29% (±0.87%)	8.52% (±3.4%)
$\left.\frac{dN}{dE}\right\|_{peak}$ (GeV^{-1})	8.2(±0.4) $\times 10^{36}$	1.08(±0.05) $\times 10^{40}$	2.0(±0.1) $\times 10^{39}$	2.36(±0.12) $\times 10^{40}$
at E_{peak} (GeV)	0.070 (±0.015)	0.022 (±0.003)	0.058 (±0.006)	0.022 (±0.003)
$\bar{E}$ (GeV)	0.255 (±0.012)	0.080 (±0.001)	0.131 (±0.001)	0.075 (±0.001)

$E' \simeq 0.2$ MeV. (The prime denotes the redshifted energy.) The redshift does not alter $dN/dE'_{p\bar{p}}$ since most $p\bar{p}$ are emitted in the present epoch. The other spectra are unaffected above $E' \simeq 0.100$ GeV, the energy at peak $T \simeq 0.02$ GeV flux. Below $E' \simeq 0.100$ GeV, $dN/dE'_{e^{\pm},\gamma,\nu\bar{\nu}}$ spreads out toward lower energies while retaining the main features. The redshifted spectra peak at 20–50% lower energies. Since N_{tot} is conserved, the heights of the peaks are about 10–40% greater. The $E^{1/2}$ to E'^{1} slope in $dN/dE'_{e^{\pm},\gamma,\nu\bar{\nu}}$ between 0.001 and 0.100 GeV comes from the peak emission of earlier epochs. The reason for the $E'^{1/2}$ slope can easily be seen: the unredshifted peak flux of a primary species from a hole at time t is independent [12] of M and occurs at $E \propto M^{-1}$. Because only the E^{-3} tail of the lifetime emission comes from the late stages of evaporation, we can take $E \propto M_i^{-1}$ for $E' \lesssim 0.1$ GeV and also estimate that $dN/dE \propto t$ at the peak. If $(1+z)$ is the redshift at emission, the peak corresponds today to $E' \propto (1+z)^{-1}E$ and so $dN/dE' = (1+z)dN/dE \propto (1+z)^{-1/2} \propto E'^{1/2}$ for

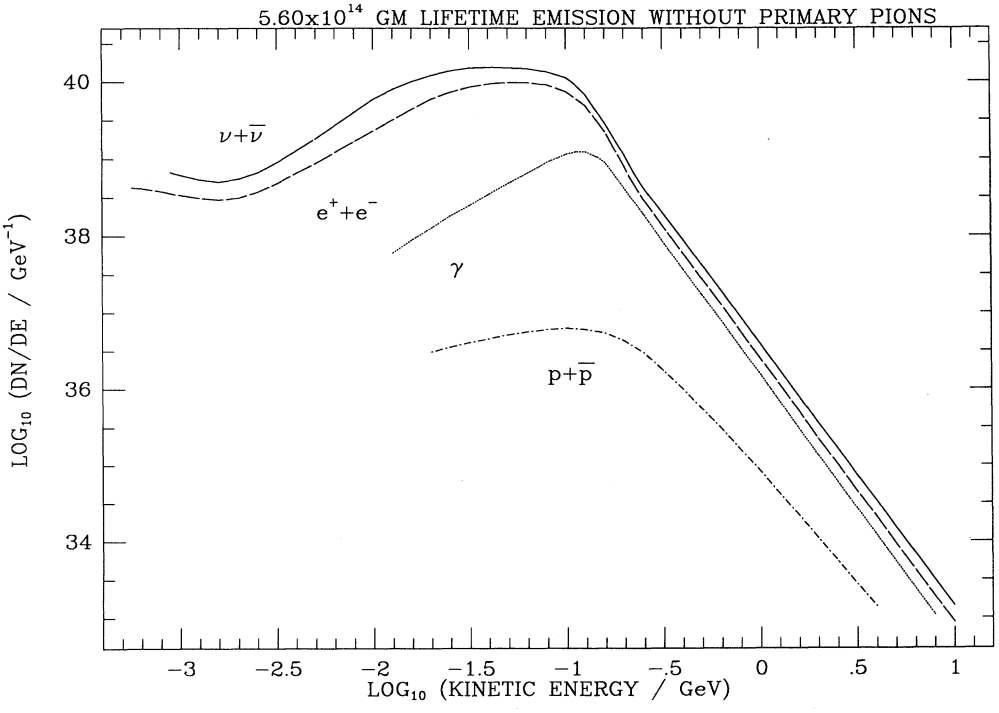

FIG. 6. The unredshifted lifetime emission from an $M_i = 5.60 \times 10^{14}$ g black hole, not emitting primary pions.

$\Omega_m = 1.0$. At later t (higher E'), particle decays are contributing to the flux and the slopes are slightly steeper than $E'^{1/2}$. The total redshifted energy is 75.1(±1.2)% of the unredshifted value. The fraction carried by jets increases to 19(±6)% since jets are emitted during the most recent epochs. The average $e^{\pm}$, γ, and $\nu\bar{\nu}$ energies are 15–30% less than the unredshifted values. These changes are consistent with noting that the $\bar{M} = 2.49(\pm 0.03)\times 10^{14}$ g hole in case (i) completes its evaporation at $(1+z)\simeq 7$ if $\Omega_m = 1.0$ and $h = 0.32$. Since the redshifted low-energy particles carry less weight in the spectra, the peaks and averages are distorted by a factor less than 7.

C. Primary pion emission

To test our sensitivity to the particle model at energies between m_π and the lowest quark masses $m_{u,d}$ we ran the unredshifted $M_i = 5.60\times 10^{14}$ g version with no primary pions, correctly adjusting $f(T)$ [see Eq. (9), Fig. 6, and Table VI]. Without the pion emission, the hole spends longer evaporating at low temperatures. $dN/dE_{p\bar{p}}$ remains unchanged, to within the statistical errors, while the $dN/dE_{e^{\pm},\nu\bar{\nu}}$ maxima double because of the greater relative contribution from primary $e^{\pm}$,$\nu\bar{\nu}$, and $\mu^{\pm}$ emission. The $dN/dE_{e^{\pm},\gamma,\nu\bar{\nu}}$ peaks, which occur at about 30–50% higher energies, are associated with the peak $T\simeq 0.02$ GeV flux. (The primary $T\simeq 0.02$ GeV flux peaks at a higher energy than the nonrelativistic pion decay). The fractions of $N_{\rm tot}$ and $E_{\rm tot}$ in each species change by less than 3% while the jet-produced fraction decreases by about 3%, since the hole spends longer at low T. $N_{\rm tot}$ increases by 7%. Although the instantaneous $T = 0.02$ GeV flux is 10–15% less if primary pions are not emitted [10], here the longer lifetime has greater influence on $N_{\rm tot}$—from Eq. (13), a black hole not emitting primary pions spends about 36% longer with its primary emission peaking between m_π and $m_{u,d}$. The smaller average energy of particles prior to decay, $\bar{Q} = 0.136(\pm 0.001)$ GeV, also reflects the prolonged emission at low temperatures. $E_{\rm tot}$, by definition, remains unchanged. The $e^{\pm}$,γ, and $\nu\bar{\nu}$ multiplicities are 7%, 44%, and 15% less, respectively, due to the lack of $\pi^{\pm,0}$ decays. In summary, the details of the particle model between 0.1 and 0.3 GeV do not significantly affect the total lifetime emission from an M_* hole. We note that any error due to our $f(M)$ approximation and use of relativistic $\Gamma_s(MQ)$ values must be less than the effect of allowing *no* primary pion emission.

D. $M_i = 7.00\times 10^{13}$ g emission

An $M_i = 7.00\times 10^{13}$ g black hole is initially emitting quarks and gluons. These account for the majority of final states. The unredshifted dN/dE spectra peak at $E\simeq 0.01$–1.0 GeV and fall off as E^{-3} at high energies, as predicted in Sec. VI (see Fig. 7 and Table VII). Below $E\simeq 0.1$ GeV, they also resemble the instantaneous

TABLE VI. Final states, total energy, spectra peaks, average multiplicities, and average kinetic energies for the lifetime emission of an $M_i = 5.60\times 10^{14}$ g hole, not emitting primary pions.

$M_i = 5.60\times 10^{14}$ g	$p\bar{p}$	$e^{\pm}$	γ	$\nu\bar{\nu}$
Number	1.75(±0.65) $\times 10^{36}$	1.11(±0.07) $\times 10^{39}$	1.82(±0.21) $\times 10^{38}$	1.90(±0.12) $\times 10^{39}$
Number (% of $N_{\rm tot}$)	0.06% (±0.02%)	34.75% (±0.87%)	5.68% (±0.43%)	59.52% (±1.27%)
		$N_{\rm tot} = 3.20(\pm 0.13)\times 10^{39}$		
Jet products (% of $N_{\rm tot}$)	0.06 (±0.02%)	1.81% (±1.51%)	2.13% (±0.65%)	5.32% (±1.21%)
$\left.\frac{dN}{dE}\right\|_{\rm peak}$ (GeV^{-1})	7.7(±0.4) $\times 10^{36}$	1.32(±0.07) $\times 10^{40}$	1.82(±0.09) $\times 10^{39}$	2.37(±0.12) $\times 10^{40}$
at $E_{\rm peak}$(GeV)	0.08 (±0.01)	0.08 (±0.01)	0.12 (±0.01)	0.041 (±0.005)
Net energy (GeV)	2.14(±0.82) $\times 10^{36}$	1.07(±0.05) $\times 10^{38}$	3.05(±0.29) $\times 10^{37}$	1.75(±0.08) $\times 10^{38}$
Energy (% of $E_{\rm tot}$)	0.68% (±0.26%)	33.99% (±1.70%)	9.68% (±0.93%)	55.65% (±2.60%)
		$E_{\rm tot} = 3.15\times 10^{38}$ GeV		
Jet products (% of $E_{\rm tot}$)	0.68% (±0.26%)	2.20% (±2%)	4.32% (±1.37%)	5.88% (±4.73%)
Multiplicities	0.001 (±0.001)	0.479 (±0.001)	0.078 (±0.001)	0.082 (±0.002)
$\bar{E}$ (GeV)	0.288 (±0.016)	0.096 (±0.001)	0.168 (±0.001)	0.092 (±0.001)

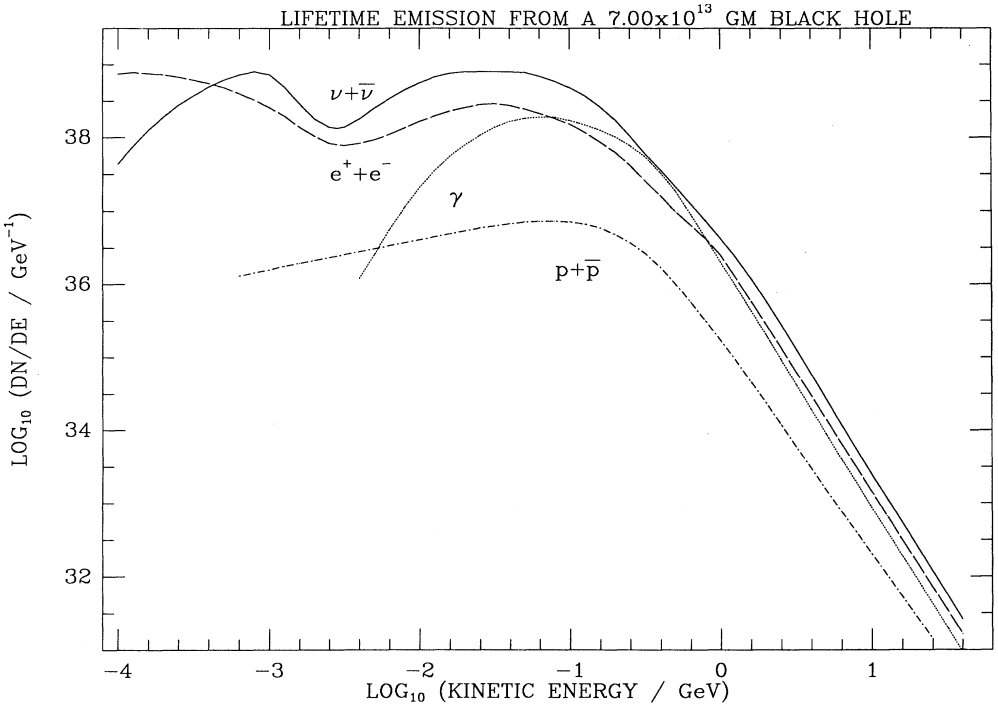

FIG. 7. The unredshifted lifetime emission from an $M_i = 7\times10^{13}$ g black hole.

$T=0.3$ GeV flux [10]. $dN/dE_{e^\pm,\gamma,\nu\bar{\nu}}$ is dominated by primary emission above $E \gtrsim 1$ GeV, with a small jet contribution, and by jet decays below $E \lesssim 1$ Gev. All protons and antiprotons are jet products. $dN/dE_{p\bar{p}}$ and possibly $dN/dE_{e^\pm,\nu\bar{\nu}}$ have the predicted E^{-1} slope at $0.1 \lesssim E \lesssim 0.2$ GeV. The $dN/dE_{e^\pm,\nu\bar{\nu}}$ peaks, which occur at energies similar to those for $M_i = M_*$, are associated with the nonrelativistic pion decays in low-energy jets. The

TABLE VII. Final states, total energy, spectra peaks, average multiplicities, and average kinetic energies for the lifetime emission of an $M_i = 7.00\times10^{13}$ g hole.

$M_i = 7.00\times10^{13}$ g	$p\bar{p}$	$e^\pm$	γ	$\nu\bar{\nu}$
Number	$2.11(\pm0.06)\times10^{36}$	$4.03(\pm0.07)\times10^{37}$	$4.01(\pm0.07)\times10^{37}$	$1.12(\pm0.02)\times10^{38}$
Number (% of $N_{\rm tot}$)	1.08% (±0.02%)	20.70% (±0.13%)	20.61% (±0.13%)	57.60% (±0.28%)
		$N_{\rm tot} = 1.94(\pm0.02)\times10^{39}$		
Jet products (% of $N_{\rm tot}$)	1.08% (±0.02%)	18.10% (±0.16%)	20.24% (±0.15%)	52.71% (±0.32%)
$\left.\frac{dN}{dE}\right\|_{\rm peak}$ ($\rm GeV^{-1}$)	$6.6(\pm0.3)\times10^{36}$	$2.51(\pm0.13)\times10^{38}$	$1.60(\pm0.08)\times10^{38}$	$8.0(\pm0.4)\times10^{38}$
at $E_{\rm peak}$ (GeV)	0.06 (±0.01)	0.027 (±0.005)	0.06 (±0.01)	0.027 (±0.005)
Net energy (GeV)	$2.67(\pm0.07)\times10^{36}$	$8.26(\pm0.14)\times10^{36}$	$9.60(\pm0.16)\times10^{36}$	$1.87(\pm0.03)\times10^{37}$
Energy (% of $E_{\rm tot}$)	6.79% (±0.18%)	21.04% (±0.36%)	24.46% (±0.40%)	47.71% (±0.80%)
		$E_{\rm tot} = 3.93\times10^{37}$ GeV		
Jet products (% of $E_{\rm tot}$)	6.79 (±0.18%)	11.61% (±0.56%)	22.72% (±0.50%)	31.76% (±1.08%)
Multiplicities	0.072 (±0.001)	1.387 (±0.001)	1.371 (±0.004)	3.832 (±0.008)
$\bar{E}$ (GeV)	0.328 (±0.004)	0.204 (±0.001)	0.240 (±0.001)	0.167 (±0.001)

bumps in $dN/dE_{e^{\pm},\nu\bar{\nu}}$ at $E \simeq 0.6-1$ GeV and below $E \simeq 0.003$ GeV are generated by the nondecaying emission and the neutron β decay, respectively. The β-decay peaks, and $dN/dE_{p\bar{p},\gamma}$ below 1 Gev, are considerably greater in relation to the rest of the spectra, than for $M_i = M_*$. dN/dE_γ now resembles the jet decay distribution, with a much greater contribution between $0.1 \lesssim E \lesssim 1.0$ GeV.

The fractions of $N_{\rm tot}$ in each species (see Table VII) resemble the values for a $T = 0.3$ GeV hole [10]. 92.1($\pm$1.3)% are jet products. $N_{p\bar{p}}$ differs little between cases (i), (ii), and (iii) because the $p\bar{p}$ are emitted at high temperatures. Although the $M_i = 7.00 \times 10^{13}$ g hole only lives about $10^{-3} t_u$, we see that $N_{\rm tot(iii)}/N_{\rm tot(i,ii)} \simeq 0.07$. Since the hole is initially emitting far more species and the multiplicities increase strongly with jets, the analysis we used in Eq. (28) to show that $N_{\rm tot}$ is determined by the $M \simeq M_i$ evaporation is not relevant here. On the other hand, if we integrate the parametrizations for the total instantaneous flux from a $T = 0.3-100$ GeV hole given in Ref. [10], $N_{\rm tot}$ is too large by a factor of $17 f(M_i)^{-1}$ for $M_i = 7 \times 10^{13}$ g. We already know [10], however, that these parametrizations are too large by a factor at $T = 0.1$ GeV because fewer primary species and decay states are emitted at low T. The average multiplicities and fractions of $E_{\rm tot} = 3.92 \times 10^{37}$ GeV carried by each species resemble the $T = 0.3$ GeV values [10] and reflect the much greater jet contribution, while the average kinetic energies are weighted to some degree by the $T \gtrsim 0.3$ GeV emission. Since 72.9($\pm$3.0)% of $E_{\rm tot}$ is carried by jets, the higher T jets must contribute significantly to $E_{\rm tot}$; the average energy of the emission, prior to decay, is 1.345($\pm$0.004) GeV and only 45% of the instantaneous power from a hole whose nondecaying emission peaks at this energy is carred by jets.

The $M_i = 7 \times 10^{13}$ g version was also run with $T_{\rm max} = 100$ GeV and $X_{\rm max} = 10$, to test our sensitivity to $T_{\rm max}$ and $X_{\rm max}$. The changes in $N_{\rm tot}$, the fractions of $N_{\rm tot}$ and $E_{\rm tot}$ in each species, and the spectra were well within the statistical errors. Since $M_i \ll M_*$, this is also an upper estimate of any variation in cases (i) and (ii). Thus, one is confident that the results in this paper truly represent the lifetime emission and do not depend on the computational cutoffs. As stated earlier, the discovery of new physics above 100 GeV can only affect the M_* lifetime emission if there are of order 10^8 new fundamental particles at 100 GeV.

IX. DISCUSSION

In this paper, the quark and gluon emission is included for the first time when deriving the lifetime emission from black holes. For $M \simeq M_*$ holes, the quark and gluon emission is significant to the final spectra. In particular it produces far more final states and a greater number of states at low energies. The quark and gluon decays dominate the emission as M decreases below M_*. This is important since an $M \lesssim M_*$ hole emits at roughly a constant redshift. The details of the particle model around $\Lambda_{\rm QH}$ do not significantly affect the final M_* spectra nor will the advent of new physics above 100 GeV.

ACKNOWLEDGMENTS

The author would like to thank Bernard Carr, Bryan Webber, and Don Page for useful discussions, and Bryan and Don for kindly supplying BIGWIG and HERWIG and the numerically generated absorption coefficient, respectively. The author is also indebted to the Fermilab Astrophysics and Theory Groups for hospitality and computer time, and Bill Press at the Harvard-Smithsonian Center for Astrophysics where part of this work was written up.

*Present address: Code 665, NASA/Goddard Space Flight Center, Greenbelt, MD 20771.

[1] B. J. Carr, in *Observational and Theoretical Aspects of Relativistic Astrophysics and Cosmology,* Proceedings of the International Course, Santander, Spain, 1984, edited by J. L. Sanz and L. J. Goicoechea (World Scientific, Singapore, 1985), p. 1.
[2] S. W. Hawking, Mon. Not. R. Astron. Soc. **152**, 75 (1971).
[3] S. W. Hawking *et al.*, Phys. Rev. D **26**, 2681 (1982); D. La and P. J. Steinhardt, Phys. Lett. B **220**, 375 (1989); M. Crawford and D. N. Schramm, Nature (London) **298**, 538 (1982).
[4] V. Canuto, Mon. Not. R. Astron. Soc. **184**, 721 (1978).
[5] S. W. Hawking, Phys. Lett. B **231**, 237 (1989); A. G. Polnarev and R. Zemboricz, Phys. Rev. D **43**, 1106 (1991).
[6] S. W. Hawking, Commun. Math. Phys. **43**, 199 (1975).
[7] S. W. Hawking, Nature (London) **248**, 30 (1974).
[8] B. J. Carr, Astrophys. J. **206**, 8 (1976).
[9] B. J. Carr, Astrophys. J. **201**, 1 (1975).
[10] J. H. MacGibbon and B. R. Webber, Phys. Rev. D **41**, 3052 (1990).
[11] D. N. Page and S. W. Hawking, Astrophys. J. **206**, 1 (1976).
[12] D. N. Page, Phys. Rev. D **13**, 198 (1976).
[13] D. N. Page, Phys. Rev. D **16**, 2402 (1977).
[14] J. H. MacGibbon (unpublished).
[15] J. H. MacGibbon and B. J. Carr, Astrophys. J **371**, 447 (1991).
[16] F. Halzen *et al.*, Nature (London) (to be published).
[17] D. N. Page, Phys. Rev. D **14**, 3260 (1976).
[18] T. Elster, J. Phys A **16**, 989 (1983); R. D. Simkins, Ph.D. thesis, Pennsylvania State University, 1986; T. Elster, Phys. Lett. **92A**, 205 (1983).
[19] F. Halzen and A. D. Martin, *Quarks and Leptons: An Introductory Course in Modern Particle Physics* (Wiley, New York, 1984), p. 243.
[20] S. Geer, in Proceedings of the PASCOS-90 Conference, Boston, Massachusetts, 1990 (unpublished).
[21] S. L. Glashow, Rev. Mod. Phys. **52**, 539 (1980).
[22] Particle Data Group, J. J. Hernandez *et al.*, Phys. Lett. B **239**, 1 (1990).
[23] J. A. Harvery *et al.*, Nucl. Phys. **B201**, 16 (1982).

[24] Mark II Collaboration, T. Barlow *et al.*, Phys. Rev. Lett. **64**, 2984 (1990); ALEPH Collaboration, D. Decamp *et al.*, Phys. Lett. B **236**, 86 (1990); OPAL Collaboration, M. Z. Akrawy *et al.*, *ibid.* **240**, 261 (1990).
[25] J. Ellis *et al.*, Nucl. Phys. **B238**, 453 (1984).
[26] K. A. Olive and J. Silk, Phys. Rev. Lett. **55**, 2362 (1985).
[27] E. W. Kolb *et al.*, Nature (London) **314**, 415 (1985).
[28] A. D. Sakharov, Pis'ma Zh. Eksp. Teor. Fiz. **44**, 295 (1986) [JETP Lett. **44**, 379 (1986)].
[29] Y. Tosa and R. E. Marshak, Phys. Rev. D **26**, 303 (1982).
[30] R. K. Kaul, Rev. Mod. Phys. **55**, 449 (1983).
[31] O. Shanker *et al.*, Nucl. Phys. **B206**, 253 (1982).
[32] S. Dimopoulos, Nucl. Phys. **B168**, 69 (1980).
[33] D. N. Page (private communcation).
[34] F. K. Thielemann, in *Relativistic Astrophysics,* Proceedings of the Thirteenth Texas Symposium, Chicago, Illinois, 1986, edited by M. P. Ulmer (World Scientific, Singapore, 1987).
[35] B. R. Webber, Nucl. Phys. **B238**, 492 (1984).
[36] G. Marchesini and B. R. Webber, Nucl. Phys. **B238**, 1 (1984).
[37] J. H. MacGibbon, Nature (London) **329**, 308 (1987).